Identifying the mechanisms underlying the protective effect of tetramethylpyrazine against cisplatin-induced *in vitro* ototoxicity in HEI-OC1 auditory cells using gene expression profiling

GUOFANG GUAN[1], XIAO HE[2], JINGJING CHEN[2], LI BIN[2] and XUXIA TANG[2]

[1]Department of Otolaryngology, The Second Hospital of Jilin University, Changchun, Jilin 130041;
[2]Department of Otolaryngology, The First Affiliated Hospital of Zhejiang Traditional Chinese Medical University, Hangzhou, Zhejiang 310006, P.R. China

Received December 28, 2019; Accepted June 26, 2020

DOI: 10.3892/mmr.2020.11631

Abstract. Sensorineural hearing loss is prevalent in patients receiving cisplatin therapy. Tetramethylpyrazine (Tet) and tanshinone IIA (Tan IIA) have protective roles against hearing impairment or ototoxicity. The present study aimed to investigate the molecular mechanisms underlying cisplatin-induced ototoxicity and the protective effect of Tet and Tan IIA against it. House Ear Institute-Organ of Corti 1 auditory cells were treated with titrating doses of Tan IIA, Tet, and cisplatin. In a cell viability assay, cisplatin, Tan IIA and Tet had IC_{50} values of 42.89 μM, 151.80 and 1.04x10^3 mg/l, respectively. Tan IIA augmented cisplatin-induced cytotoxicity. However, Tet concentrations <75 mg/l attenuated cisplatin-induced cytotoxicity and apoptosis. Moreover, RNA sequencing analysis was carried out on auditory cells treated for 30 h with 30 μM cisplatin alone for 48 h or combined with 37.5 mg/l Tet for 30 h. Differentially expressed genes (DEGs) induced in these conditions were identified and examined using Gene Ontology and Kyoto Encyclopedia of Genes and Genomes pathway analysis. Cisplatin increased the expression of genes related to the p53 and FoxO pathways, such as Fas, p21/CDKN1A, and Bcl-2 binding component 3, but decreased the expression of insulin-like growth factor 1 (IGF1), as well as genes in the histone (Hist)1 and Hist2 clusters. Treatment with Tet downregulated FOXO3 and Bcl-2 binding component 3, and increased the expression of IGF1. Moreover, Tet upregulated genes associated with Wnt signaling, but not p53-related genes. Thus, the otoprotective properties of Tet might be mediated by activation of Wnt and IGF1 signaling, and inhibition of FoxO signaling.

Correspondence to: Dr Xuxia Tang, Department of Otolaryngology, The First Affiliated Hospital of Zhejiang Traditional Chinese Medical University, 54 Youdian Road, Hangzhou, Zhejiang 310006, P.R. China
E-mail: maggietangzj@163.com

Key words: sensorineural hearing loss, ototoxicity, cisplatin, tanshinone, tetramethylpyrazine, transcriptome

Introduction

Cisplatin is a radiation sensitizer and cytotoxic agent commonly used in cancer therapy. Cisplatin-induced sensorineural hearing loss (SHL) is especially prevalent among patients with brain tumors, head and neck cancer, and nasopharyngeal carcinoma (1-3). The incidence of low- and high-frequency SHL ranges from 10-97% in patients who receive cisplatin-based chemoradiation (2-4). Despite recent advances in treatments for cisplatin-induced SHL, the prevalence of cisplatin-induced cytotoxicity and damage in cochlear hair cells remains high (3). The primary cisplatin accumulation site is the cochlea, where cisplatin can be retained for months, or even years (1). As a result, the time from cisplatin chemotherapy to SHL onset also ranges from months to years (5).

Cisplatin-induced SHL is mechanistically related to enhanced apoptosis and DNA damage (6,7). It has also been reported that reactive oxygen species (ROS), as well as Wnt and p53 signaling pathways, are activated in the cochlea following cisplatin therapy (8-10). Wnt activation protects against cytotoxicity in cochlear hair cells (9). Moreover, abnormal expression of genes and non-coding RNAs, such as microRNAs, is also associated with SHL (11).

Several drugs with antagonistic effects against cisplatin-induced cytotoxicity, DNA damage, and apoptosis in cochlear hair cells might represent potential treatment strategies for cisplatin-induced ototoxicity (10,12-14). For instance, tetramethylpyrazine (Tet) and tanshinone IIA (Tan IIA) can protect against hearing impairment and ototoxicity induced by aminoglycoside antibiotics, cisplatin, and radiation (15-17). Tet can also decrease caspase-3 expression in spiral ganglion and apoptosis in guinea pig cochlea (15,17). Tan IIA has been reported to protect House Ear Institute-Organ of Corti 1 (HEI-OC1) auditory cells from cisplatin-induced ototoxicity and may synergize with cisplatin, enhancing cytotoxicity against cancer cells by promoting apoptosis and cell cycle arrest at the S phase (18).

The molecular mechanisms underlying the protective effects of Tet and Tan IIA against cisplatin-induced ototoxicity are poorly understood. Therefore, the aim of the present study was to determine the mechanistic basis of this otoprotective effect *in vitro*. HEI-OC1 auditory cells were exposed to cisplatin and treated with Tet or Tan IIA. Tet, but not Tan IIA, reversed the inhibitory effect of cisplatin on HEU-OC1 viability. The underlying molecular mechanisms were investigated using high-throughput, next-generation sequencing, and bioinformatics analysis. The findings of the present study provided insight into cisplatin-induced ototoxicity *in vitro* and the Tet-mediated protective effects against it.

Materials and methods

Cell culture. HEI-OC1 auditory cell line was a gift from Professor Federico Kalinec (David Geffen School of Medicine at UCLA, CA, USA) and maintained at 32˚C in 10% CO_2 in high-glucose Dulbecco's modified Eagle's medium (DMEM; HyClone; GE Healthcare Life Sciences) supplemented with 2 mM L-glutamine, 1 mM sodium pyruvate and 10% fetal bovine serum (FBS; HyClone).

Cell treatments. HEI-OC1 auditory cells were separately treated for 48 h at 32˚C in 10% CO_2 with Tan IIA (3, 9, 27, 81, 243 or 729 mg/l; Shanghai Yuanye Biotechnology Co., Ltd.), Tet (125, 250, 500, $1x10^3$, $2x10^3$, 4 10^3, $8x10^3$ or $1.60x10^4$ mg/l; Shanghai Aladdin Bio-Chem Technology Co., Ltd.) or cisplatin (5, 10, 20, 40, 80 and 160 μM; Sigma-Aldrich; Merck KGaA). In a separate experiment, the cells were treated for 30 h with 30 μM cisplatin combined either with Tan IIA (0.2, 0.5, 1.0, or 1.5 mg/l) or with Tet (37.5, 75, 125 or 250 mg/l) at 32˚C in 10% CO_2. The assays were carried out in triplicate wells.

Cell viability assay. Cells were seeded into 96-well plates (Corning, Inc.) at a density of $5x10^4$ cells/ml and maintained in high-glucose DMEM for 24 h. The culture medium was then replaced with fresh medium supplemented with Tan IIA, Tet, cisplatin or combinations as aforementioned. Cell viability was then assessed using Cell Counting Kit-8 (MedChemExpress) according to the manufacturer's instructions. The optical density was read at 450 nm using a microplate reader (Bio-Rad Laboratories, Inc.).

Cell apoptosis assay. Cell apoptosis was measured using Annexin V-fluorescein isothiocyanate (FITC) and propidium iodide (PI; Beyotime Institute of Biotechnology) staining. Cells ($5x10^4$ cells/well) were plated in 6-well plates, then treated in triplicate with cisplatin for 48 h or with cisplatin and Tet for 30 h at 32˚C in 10% CO_2. Following incubation, cells were collected by centrifugation at 4˚C and 1,500 x g for 5 min, then resuspended in 1X binding buffer. The samples were then stained with 5 μl of Annexin-V-FITC solution and 5 μl of PI at 4˚C for 10-15 min in dark. The data were acquired using a BD FACSCanto-II flow cytometer (BD Biosciences) and analyzed using an Olympus BX51 fluorescence microscope (Olympus Optical, Tokyo, Japan).

Western blot analysis. Proteins were extracted using RIPA lysis buffer (Beyotime Institute of Biotechnology) according to the manufacturer's instructions. Protein concentration was determined using a Bradford protein assay kit (Thermo Fisher Scientific Inc.). The samples (20 μg) were resolved by SDS-PAGE on 10% gels (Shanghai Sangong Pharmaceutical Co., Ltd.), then transferred to PVDF membranes (EMD Millipore). The membranes were then blocked with 5% nonfat milk (Beyotime Institute of Biotechnology) at room temperature for 1 h. The membranes were first incubated with target-specific primary antibodies, including anti-P21 (1:1,000; cat. no. ab188224; Abcam), anti-p16-INK4A (1:1,000; cat. no. ab211542; Abcam), anti-FOXO3 (1:1,500; cat. no. 2497S; Cell Signaling Technology, Inc.), anti-caspase 3 (1:1,000; cat. no. ab13847; Abcam), anti-Fas (1:2,000; cat. no. ab216991; Abcam), anti-Wnt receptor frizzled 6 (FZD6; 1:2,000; cat. no. DF4930; Affinity Biosciences), anti-transcriptional repressor transcription factor 7-like 1 (TCF7L1; 1:1,500; cat. no. ab86175; Abcam), anti-wingless-type MMTV integration site family, member 2 (WNT2; 1:800; cat. no. ab109222; Abcam), anti-insulin-like growth factor 1 (IGF1; 1:1,500; cat. no. ab182408; Abcam), anti-SERPINE1 (1:1500; cat. no. DF13553; Affinity Biosciences) and anti-GAPDH (1:10,000; cat. no. KC-5G5; Shanghai Kangcheng Biotechnology Co. Ltd.) at 4˚C overnight. The membranes were then incubated with horseradish peroxidase-conjugated secondary antibody (anti-rabbit IgG; 1:20,000; cat. no. ba1054; Boster Biological Technology, Ltd.) at room temperature for 40 min. Lastly, protein bands were visualized using an ECL kit (EMD Millipore).

RNA extraction and whole transcriptome sequencing. Total RNA was extracted using the TRIzol® reagent (Invitrogen; Thermo Fisher Scientific, Inc.) at 48 and 30 h post-treatment. RNA concentration and purity were determined using a NanoDrop 2000 spectrophotometer (Thermo Fisher Scientific, Inc.) and an Agilent 2100 Bioanalyzer (Agilent Technologies Inc.). RNA samples with an RNA integrity number (RIN) value of > eight were used for library preparation. RNA was fragmented, reverse transcribed to the first-strand cDNA using reverse transcriptase (Invitrogen; Thermo Fisher Scientific, Inc.) and random hexamers (Sangon Biotech Co., Ltd.), then synthesized to double-stranded DNA using dNTPs (Invitrogen; Thermo Fisher Scientific, Inc.) at 37˚C for 15 min and at 98˚C for 5 min. The DNA sequencing libraries were prepared using a TruSeq™ RNA Sample Preparation Kit (version 2; Illumina, cat. nos. RS-122-2001 RS-122-2002) following the protocols including DNA fragment end repair, adenylating, adapter ligation, and fragment amplification. After verifying the library quality using the Qubit2.0 (Thermo Fisher Scientific, Inc.), Agilent 2100 (Agilent Technologies Inc.), and qPCR, sequencing (loading concentration 3 nM/μl) was carried out using a V1 sequencing kit (Illumina, Inc.) on an Illumina HiSeq 4000 sequencing platform (paired-end; 150 bp; Illumina, Inc.).

Data processing. Base calling of the original sequencing image data and fastq file extraction were carried out using Illumina CASAVA software (version 1.8.2; Illumina, Inc.). The quality of raw data was checked using the FastQC program (version 0.11.5; http://www.bioinformatics.babraham.

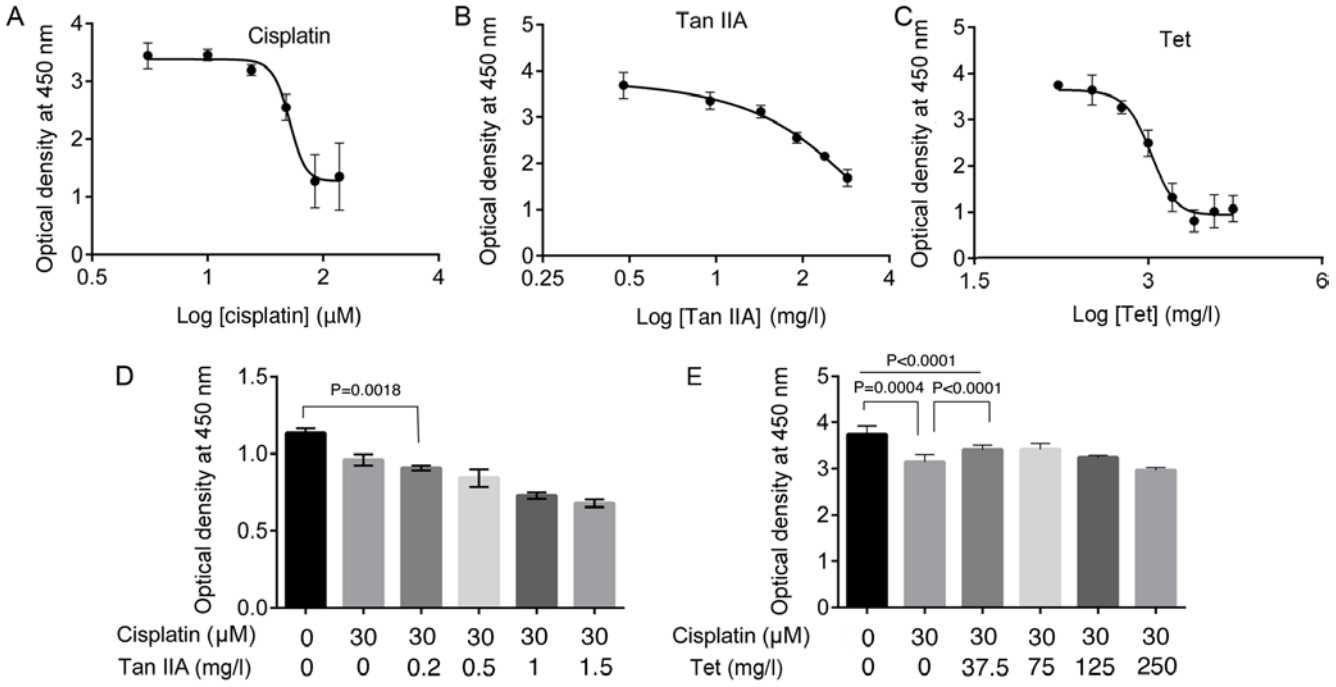

Figure 1. Cisplatin, Tan IIA and Tet inhibit the viability of HEI-OC1 cells. (A-C) Dose-dependent inhibition of viability of HEI-OC1 cells following 48-h treatment with cisplatin, Tan IIA and Tet. HEI-OC1 cell viability following 30-h treatment with (D) Cisplatin + Tan IIA or (E) Cisplatin + Tet. Differences among groups in panel D and E were analyzed using one-way ANOVA followed by Tukey's post hoc test. Tan IIA, tanshinone IIA; Tet, tetramethylpyrazine.

ac.uk/projects/fastqc/). After adaptor trimming and removal of duplicated and low-quality reads (unknown base sequence >10%, and >50% of the read consisted of reads with Phred scores of ≤3) using Trimmomatic (version 0.30; http://www.usadellab.org/cms/?page=trimmomatic), the clean reads were mapped to the ENSEMBL *Mus musculus* GRCm38.p6 reference genome (http://www.ensembl.org/) with annotation version GRCm38.97 using the TopHat 2 software (http://ccb.jhu.edu/software/tophat/index.shtml).

Transcript assembly and quantification was performed using the Cufflinks software (version 2.2.1; http://cufflinks.cbcb.umd.edu/) by calculating the expected number of fragments per kilobase of exon model per million reads mapped (FPKM) values in each sample. Differentially expressed genes (DEGs) between groups were identified using the edgeR statistical software package (Bioconductor; http://www.bioconductor.org/) according to the criteria of FDR <0.05 and $|\log_2(FC)|\geq 1$, where FDR is the false discovery rate and FC is the fold change.

Enrichment analysis. Gene Ontology (GO; http://www.geneontology.org/) biological processes and Kyoto Encyclopedia of Genes and Genomes (KEGG) pathways associated with the DEGs were identified from the Database for Annotation, Visualization, and Integrated Discovery (DAVID; version 6.7; http://david.ncifcrf.gov/). P<0.05 was used to identify statistically significant terms.

Protein-protein interaction (PPI) network analysis. The interaction between DEGs was predicted and extracted from STRING (version 10; www.string-db.org). PPI networks were constructed and visualized using Cytoscape (version 2.8; http://www.cytoscape.org/).

Statistical analysis. Quantitative data are presented as the mean ± SD of triplicates. Statistical analysis was carried out using GraphPad Prism software (version 6; GraphPad Software, Inc.). Multigroup comparisons were analyzed using one-way ANOVA followed by Tukey's post hoc test. The IC_{50} values of Tan IIA, Tet, and cisplatin were calculated using nonlinear regression. P<0.05 was considered to indicate a statistically significant difference.

Results

Cisplatin, Tan IIA, and Tet inhibit HEI-OC1 auditory cell viability. Treatment with cisplatin, Tan IIA, and Tet for 48 h inhibited the viability of HEI-OC1 auditory cells in a dose-dependent manner (Fig. 1A-C), with IC_{50} values of 42.89 μM, 151.80 and $1.04x10^3$ mg/l, respectively.

Low Tet concentration prevents cisplatin-induced cytotoxicity in HEI-OC1 auditory cells. To investigate whether Tan IIA and Tet administration could suppress the inhibitory effect of cisplatin on HEI-OC1 auditory cell viability, cells were treated with 30 μM cisplatin combined with Tan IIA (0.2, 0.5, 1.0 and 1.5 mg/l) or Tet (37.5, 75, 125 and 250 mg/l) for 30 h. To minimize drug-related cytotoxicity, the selected concentrations were <IC_{50} values. The addition of Tan IIA at concentrations <1.5 mg/l augmented the effect of cisplatin and further inhibited viability significantly compared with cisplatin alone (P=0.0018, Fig. 1D). However, at concentrations of 37.5 and 75 mg/l Tet significantly increased viability, compared with cisplatin alone (P<0.0001, Fig. 1E).

The percentage of apoptotic HEI-OC1 auditory cells was significantly increased following cisplatin treatment, compared with control cells (10.27±0.64% and 3.11±0.17% in the second

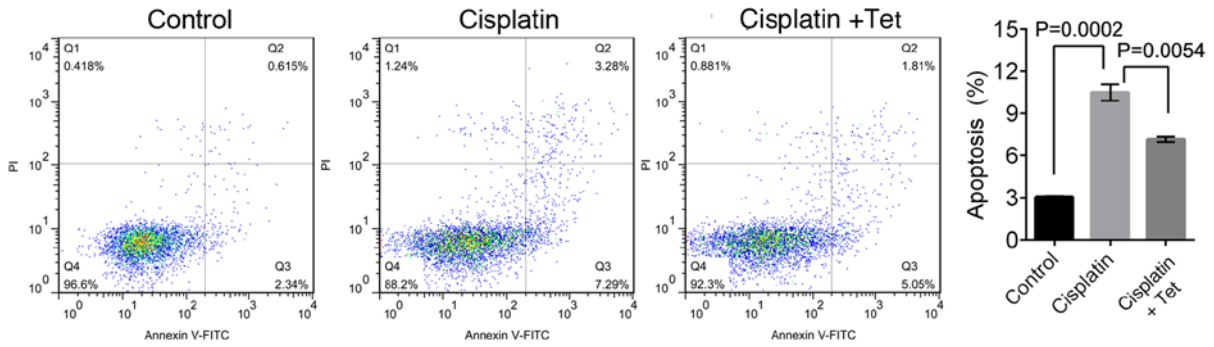

Figure 2. Apoptosis of HEI-OC1 cells. HEI-OC1 cells were treated with cisplatin alone or combined with Tet. Differences between groups were analyzed using one-way ANOVA followed by Tukey's post hoc test. PI, propidium iodide; FITC, fluorescein isothiocyanate; Tet, tetramethylpyrazine.

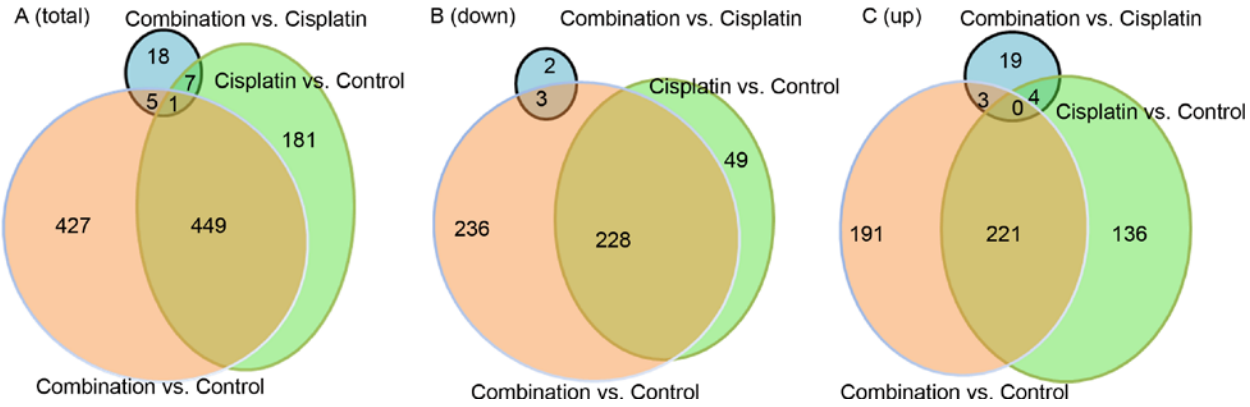

Figure 3. The Venn diagram of DEG in HEI-OC1 cells. (A-C) Venn diagram of the (A) total, (B) downregulated, and (C) upregulated DEGs identified following treatment with cisplatin alone or combined with Tet. DEG, differentially expressed gene.

(upper right) and third (lower right) quadrants, respectively; P=0.0002; Fig. 2). However, co-treatment with cisplatin and Tet reduced the apoptosis rate to 7.18±0.33% (P=0.0054). Collectively, these results indicated that low concentrations of Tet could protect HEI-OC1 cells against cisplatin-induced cytotoxicity.

Summary of Illumina sequencing. To examine the molecular mechanisms associated with the otoprotective properties of Tet, RNA sequencing (RNA-seq) analysis was carried out on HEI-OC1 auditory cells treated with 30 μM cisplatin alone or combined with 37.5 mg/l Tet. Illumina sequencing produced a total of 518.83 million raw reads, corresponding to 510.65 million clean reads and 74.31 Gbp (Table SI). The average GC content was 50.26%, while the average frequency of reads >Q30 was 95.91%. Transcriptome assembly generated 1,455,306 transcripts. In comparison with control cells, 638 DEGs were identified following cisplatin treatment, including 361 upregulated genes and 277 downregulated genes (Fig. 3A-C). Moreover, 882 DEGs were observed in cells treated with a combination of cisplatin and Tet, including 415 upregulated and 467 downregulated genes (Fig. 3B and C). Thus, relative to untreated cells, the combination of cisplatin and Tet induced more DEGs than cisplatin alone. A total of 449 DEGs were shared between the two datasets, including 221 upregulated and 228 downregulated DEGs (Fig. 3B and C). In comparison with cisplatin alone, the combination with Tet (37.5 mg/l) only induced 31 DEGs, including 26 upregulated and 5 downregulated DEGs). In total, 1,088 DEGs were identified, including 626 non-overlapping DEGs (Fig. 3A-C).

Summary and annotation of cisplatin-induced DEGs. To examine the molecular mechanisms underlying cisplatin-induced cytotoxicity, the biological processes and pathways associated with the identified DEGs were examined using GO and KEGG analysis. GO functional enrichment analysis indicated that downregulated DEGs, such as histone (Hist)1 and Hist2 gene clusters (Fig. 4), were associated with biological processes related to 'DNA replication-dependent nucleosome assembly', 'nucleosome assembly', and 'DNA-templated transcription, initiation' (Table I). Other downregulated DEGs were also associated with biological processes, including 'negative regulation of apoptotic process' (thrombospondin1, THBS1; TWIST2; insulin-1 receptor antagonist gene, IL1RN; IGF1) and regulation of cell migration (IL1RN; SERPINE1; IGF binding protein 5, IGFBP5).

Moreover, the downregulated DEGs identified following cisplatin treatment were also associated with several KEGG pathways. Genes in the Hist1 and Hist2 clusters were associated with 'Systemic lupus erythematosus', 'Alcoholism' and 'Viral carcinogenesis' (Table II). IGF1 and THBS1 were involved in 'PI3K-Akt signaling pathway', 'Rap1 signaling pathway', and 'HIF-1 signaling pathway'.

Notably, the upregulated DEGs induced by cisplatin in HEI-OC1 auditory cells were significantly associated with autophagy (autophagy-related gene 12, ATG12; ATG9B;

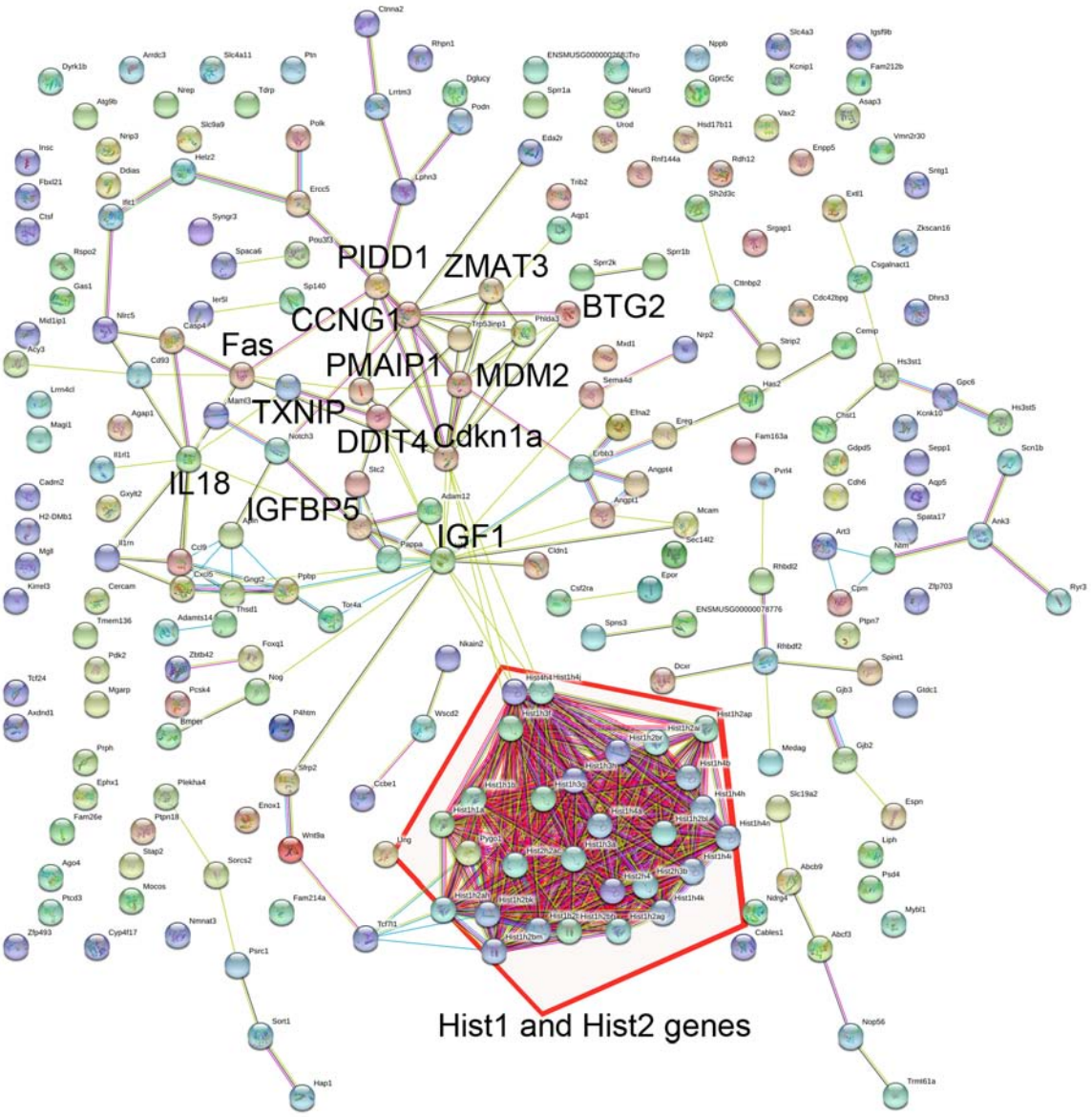

Figure 4. Protein-protein interaction network of the identified DEGs. The protein-protein interaction network consists of 364 nodes (gene products) and 1,268 lines (interaction pairs). DEG, differentially expressed gene.

ATG2A), apoptosis-associated processes, response to DNA damage and cell cycle arrest. These genes included phorbol-12-myristate-13-acetate-induced protein 1 (PMAIP1), Bcl-2 binding component 3 (BBC3), zinc finger matrin-type 3 (ZMAT3), p53-induced death domain protein 1 (PIDD1), B-cell translocation gene protein 2 (BTG2), thioredoxin-interacting protein (TNXIP), DNA damage induced apoptosis suppressor (DDIAS), cycle-dependent kinase inhibitor 1A (CDKN1A), transformation related protein 53-induced nuclear protein 1 (TRP53INP1), FOXO3, and Fas (Table I). These DEGs interacted closely (Fig. 4) and some (including CDKN1A, BBC3, ZMAT3, PMAIP1, FAS, PIDD1, and FOXO3) were significantly associated with 'p53 signaling pathway' and 'FoxO signaling pathway' (Table II).

Common effect of Tet and cisplatin on transcriptome expression profiles. As indicated in Fig. 3, 450 DEGs were shared between the two treatments. The shared DEGs included Fas, PMAIP1, ATG12, CDKN1A, and ZMAT3, which were upregulated, and THBS1 and SERPINE1, which were downregulated (Fig. 5A-D). Enrichment analysis showed these shared genes enriched in similar functional categories and KEGG pathways as DEGs induced by cisplatin alone (Tables III and IV). The upregulated genes including THBS1, CDKN1A, Fas, PMAIP1, TXNIP, and ZMAT3 were associated with biological processes, such as 'programmed cell death' and 'cell cycle' (Table III). Genes including CDKN1A, Fas, PMAIP1, TXNIP, and ZMAT3 and pathways including 'p53 signaling pathway' and/or 'Apoptosis' (Table IV). The downregulated genes including the histone genes, endothelin 1 (EDN1), suppressor of cytokine signaling 3 (SOCS3), and insulin receptor substrate 1 (IRS1) were associated with biological processes, such as 'nucleosome assembly' and 'regulation of phosphate metabolic process' (Table III). The downregulated DEGs including THBS1, collagen type III alpha 1 chain (COL3A1), and platelet derived growth factor subunit B (PDGFB) were involved in 'ECM-receptor interaction' and 'Focal adhesion' (Table IV).

Table I. Top 15 GO biological processes associated with the differentially expressed genes induced by cisplatin vs. control.

A, Downregulated genes

Term	Count	P-value	Gene name
GO:0006334, nucleosome assembly	24	3.3010^{-22}	HIST2H3B, HIST1H2BB, HIST1H1C, HIST1H1B, H1F0, ANP32B, H3F3B, HIST1H3F, HIST1H4I, HIST1H3G, etc.
GO:0000183, chromatin silencing at rDNA	16	$2.22\text{x}10^{-16}$	HIST2H3B, HIST1H2BB, HIST1H1C, HIST1H1B, BEND3, POLR1B, HIST2H4, SAP30, UBTF, HIST1H4A, etc.
GO:0032776, DNA methylation on cytosine	12	$1.37\text{x}10^{-13}$	HIST2H3B, HIST4H4, HIST1H4A, HIST1H4B, HIST1H3A, H3F3B, HIST1H3F, HIST1H4I, HIST1H3G, HIST1H4J, etc.
GO:0045815, positive regulation of gene expression, epigenetic	12	$2.03\text{x}10^{-13}$	HIST2H3B, HIST4H4, HIST1H4A, HIST1H4B, HIST1H3A, H3F3B, HIST1H3F, HIST1H4I, HIST1H3G, HIST1H4J, etc.
GO:0006335, DNA replication-dependent nucleosome assembly	11	$7.75\text{x}10^{-12}$	HIST2H3B, HIST4H4, HIST1H4A, HIST1H4B, HIST1H3A, HIST1H3F, HIST1H4I, HIST1H3G, HIST1H4J, HIST1H4H, etc.
GO:0051290, protein heterotetramerization	11	$3.70\text{x}10^{-10}$	HIST2H3B, HIST4H4, HIST1H4A, HIST1H4B, HIST1H3A, HIST1H3F, HIST1H4I, HIST1H3G, HIST1H4J, HIST1H4H, etc.
GO:0006336, DNA replication-inde pendent nucleosome assembly	8	$2.19\text{x}10^{-8}$	HIST4H4, HIST1H4A, HIST1H4B, H3F3B, HIST1H4I, HIST1H4J, HIST1H4H, HIST2H4
GO:0045653, negative regulation of megakaryocyte differentiation	7	$4.84\text{x}10^{-8}$	HIST4H4, HIST1H4A, HIST1H4B, HIST1H4I, HIST1H4J, HIST1H4H, HIST2H4
GO:0001649, osteoblast differentiation	12	$2.46\text{x}10^{-7}$	NOG, IGF1, COL6A1, TWIST2, IGFBP5, SPP1, FHL2, GJA1, H3F3B, MYBBP1A, etc.
GO:0043066, negative regulation of apoptotic process	25	$3.61\text{x}10^{-7}$	TWIST2, THBS1, IL1RN, IGF1, GAS1, SERPINB9, PDGFRB, YBX3, FHL2, AQP1, etc.
GO:0001701, in utero embryonic development	17	$1.89\text{x}10^{-6}$	NOG, EDN1, YBX3, TPM1, HES1, PDGFRB, ANGPT1, PTCH1, GJB3, GJA1, etc.
GO:0030324, lung development	11	$4.89\text{x}10^{-6}$	HES1, MIR92-1, MIR17, MIR18, CCBE1, MIR20A, PTN, IGF1, LOX, MIR19B-1, etc.
GO:0006352, DNA-templated transcription, initiation	7	$7.32\text{x}10^{-6}$	HIST4H4, HIST1H4A, HIST1H4B, HIST1H4I, HIST1H4J, HIST1H4H, HIST2H4
GO:0030336, negative regulation of cell migration	10	$9.64\text{x}10^{-6}$	NOG, PDGFB, SFRP2, IL1RN, SERPINE1, PTN, CNN2, TPM1, SRGAP1, IGFBP5
GO:0030335, positive regulation of cell migration	13	$1.38\text{x}10^{-5}$	PDGFB, EDN1, IGF1, AQP1, CXCL12, THBS1, IRS1, CEMIP, SEMA3C, PDGFRB, etc.

B, Upregulated genes

Term	Count	P-value	Gene name
GO:0006914, autophagy	9	$1.97\text{x}10^{-4}$	TRP53INP1, ATG9B, ATG12, ATG2A, SESN2, HAP1, ABARAPL1, OPTN, ARSA
GO:0006915, apoptotic process	18	$2.35\text{x}10^{-4}$	ZMAT3, FOXO3, PMAIP1, TRP53INP1, BBC3, PIDD1, FAS, DDIAS, DDIT4, PHLDA3, etc.
GO:0072332, intrinsic apoptotic signaling pathway by p53 class mediator	5	$3.76\text{x}10^{-4}$	PDK2, BBC3, ZMAT3, EDA2R, PMAIP1
GO:0042771, intrinsic apoptotic signaling pathway in response to DNA damage by p53 class mediator	5	$3.76\text{x}10^{-4}$	CDKN1A, BBC3, PMAIP1, PHLDA3, DDIT4
GO:0006919, activation of cysteine-type endopeptidase activity involved in apoptotic process	6	$9.12\text{x}10^{-4}$	TNFRSF10B, NOD1, BBC3, PMAIP1, APAF1, PIDD1
GO:0006974, cellular response to DNA damage stimulus	14	$9.13\text{x}10^{-4}$	CDKN1A, BBC3, TRP53INP1, PIDD1, PMAIP1, DDIAS, BTG2, ZMAT3, ERCC5, POLK, etc.

Table I. Continued.

B, Upregulated genes

Term	Count	P-value	Gene name
GO:0000045, autophagosome assembly	5	$1.45x10^{-3}$	ATG9B, GABARAPL1, ATG12, ATG2A, TRP53INP1
GO:0048536, spleen development	5	$1.7x10^{-3}$	RIPK3, NFKB2, FAS, CTC1, RC3H1
GO:0007050, cell cycle arrest	6	$2.13x10^{-3}$	CDKN1A, AK1, RASSF1, WDR6, TRP53INP1, DDIAS
GO:0016236, macroautophagy	4	$2.34x10^{-3}$	ATG12, NBR1, OPTN, ZFYVE1
GO:0051607, defense response to virus	8	$2.75x10^{-3}$	DDX58, NLRC5, IFIT1, TMEM173, PMAIP1, EIF2AK2, CXCL10, DDIT4
GO:0006977, DNA damage response, signal transduction by p53 class mediator resulting in cell cycle arrest	3	$4.25x10^{-3}$	CDKN1A, MDM2, PIDD1
GO:0043029, T cell homeostasis	4	$4.90x10^{-3}$	RIPK3, PMAIP1, FAS, RC3H1
GO:0000422, mitophagy	4	$6.37x10^{-3}$	ATG9B, GABARAPL1, ATG12, ATG2A
GO:0070059, intrinsic apoptotic signaling pathway in response to endoplasmic reticulum stress	4	$7.48x10^{-3}$	TNFRSF10B, BBC3, PMAIP1, APAF1

GO, Gene Ontology.

Specific effect of cisplatin and Tet combination on HEI-OC1 auditory cells. Of the 882 DEGs induced by the cisplatin and Tet combination, the 467 downregulated histone genes were involved in biological processes including 'nucleosome assembly' and 'nucleosome organization' (Table V), and one KEGG pathway of 'Systemic lupus erythematosus' (Table VI). The downregulated DEGs that were specifically induced by combination treatment, including cyclin-dependent kinase inhibitor 2A (CDKN2A) were related to biological processes like 'rRNA processing' and 'ncRNA metabolic process' (Table V). The downregulated CCND1 specifically responded to combination treatment was also involved in 'Focal adhesion' (Table VI).

The 415 upregulated genes (such as ZMAT3, PMAIP1, TRP53INP1, CDKN1A, BTG2, and FAS) were clustered in biological processes including 'programmed cell death', 'cell cycle', 'induction of apoptosis' and 'apoptosis' (Table V), as were the DEGs that were specifically upregulated by the combination treatment (including Caspase-3 (CASP3) and IL18 (Table V). Genes like CDKN1A, CASP3, ZMAT3, PMAIP1, and FAS were involved in 'p53 signaling pathway', and genes including CASP3, CDKN1A, and FAS were related to 'pathways in cancer', as were TCF7L1 and FZD6 genes that were specifically responded to combination treatment (Table VI).

Most of the 432 DEGs that were specifically induced by the combination treatment were associated with the biological processes and KEGG pathways that were similar to the functional categories associated with the 882 DEGs related to combination treatment (Table SII). For instance, downregulated genes including CDKN2A were related to the biological processes that related to the metabolism and biogenesis of ribosome and nucleosome, and the processing of RNAs (Table SII). upregulated CASP3 and IL18, were associated with 'positive regulation of apoptotic process' and 'positive regulation of cell death'. The 'Pathways in cancer' pathway enriched upregulated WNT9A, TCF7L1, and FZD6 (Table SII).

The expression patterns of several DEGs are shown in Fig. 5. The FPKM of ATG12, ATG2A, ZMAT3, DDIAS, TRP53INP1, TXNIP, CDKN1A, BTG2, PMAIP1, PIDD1 and Fas increased following treatment with cisplatin alone or in combination with Tet, compared with untreated control cells. By contrast, serpine1, THBS1 and IGFBP5 were downregulated.

The expression of IGF1 (Fig. 5B) decreased following cisplatin treatment but was rescued by the addition of Tet ($P<0.05$). FOXO3 expression followed the opposite pattern (Fig. 5C). In comparison with control and cisplatin alone, Tet treatment increased the expression of caspase 3, IGF2R, FZD6, IL18, TCF7L1, and decreased the expression of WNT2/4, CCND1 and CDKN2A (Fig. 5B and C). The gene expression changes induced specifically by Tet, and their associated biological processes, may serve an important role in inhibiting cisplatin-induced cytotoxicity in HEI-OC1 auditory cells.

Validation of protein expression. Protein expression of several DEGs was determined using western blot analysis. CDKN1A/p21 and Fas upregulation was cisplatin-dependent and Tet-independent (Fig. 5E). However, expression of CDKN2A/p16-INK4A and WNT2 were decreased, whereas TCF7L1, FZD6, and CASP3 were specifically upregulated by the combination of cisplatin and Tet.

Discussion

Cisplatin-associated ototoxicity is a major complication of cisplatin-based chemotherapy (2,3,5). Cisplatin-induced

Table II. Kyoto Encyclopedia of Genes and Genomes pathways associated with the differentially expressed genes induced by cisplatin vs. control.

A, Downregulated genes

Term	Count	P-value	Gene name
mmu05322, Systemic lupus erythematosus	26	7.48×10^{-19}	HIST1H2AF, HIST1H2AG, HIST1H2BM, HIST1H4A, HIST1H2BK, HIST1H4B, HIST1H2BL, HIST2H2AC, HIST1H2BJ, HIST3H2A, etc.
mmu05034, Alcoholism	26	2.04×10^{-15}	HIST1H4A, HIST1H2BK, HIST1H4B, HIST1H2BL, HIST2H2AC, HIST1H2BJ, HIST3H2A, H2AFX, HIST1H4I, HIST1H4J, etc.
mmu05203, Viral carcinogenesis	15	2.98×10^{-5}	HIST1H2BB, HIST4H4, HIST1H2BH, HIST2H4, HIST1H2BM, MRPS18B, HIST1H4A, HIST1H2BK, HIST1H4B, HIST1H2BL, etc.
mmu04510, Focal adhesion	11	2.43×10^{-3}	PDGFB, TLN2, COL1A2, PDGFRB, IGF1, THBS1, COL5A3, SPP1, PDGFC, COL3A1, SPP1, etc.
mmu05202, Transcriptional misregulation in cancer	9	6.42×10^{-3}	MAF, HIST2H3B, HIST1H3A, IGF1, PBX1, HIST1H3G, ID2, H3F3B, HIST1H3F,
mmu05206, MicroRNAs in cancer	12	6.50×10^{-3}	PDGFB, PDGFRB, MARCKS, THBS1, IRS1, TPM1, MIR17, MIR18, MIR20A, etc.
mmu04151, PI3K-Akt signaling pathway	13	1.45×10^{-2}	PDGFB, PDGFRB, IGF1, ANGPT1, THBS1, IRS1, ANGPT4, SPP1, COL5A3, COL3A1, etc.
mmu04512, ECM-receptor interaction	6	1.59×10^{-2}	COL3A1, COL1A2, COL6A1, THBS1, COL5A3, SPP1
mmu04015, Rap1 signaling pathway	9	2.72×10^{-2}	PDGFB, TLN2, IGF1, ANGPT1, THBS1, ANGPT4, MAGI1, PDGFRB, PDGFC
mmu04066, HIF-1 signaling pathway	6	2.81×10^{-2}	EDN1, SERPINE1, HK2, IGF1, ANGPT1, ANGPT4
mmu04330, Notch signaling pathway	4	4.86×10^{-2}	DTX4, HES1, MAML3, LFNG

B, Upregulated genes

Term	Count	P-value	Gene name
mmu04115, p53 signaling pathway	12	1.77×10^{-10}	CDKN1A, BBC3, ZMAT3, MDM2, PMAIP1, FAS, CCNG1, PIDD1, SESN2, CCNG2, etc.
mmu05169, Epstein-Barr virus infection	8	8.93×10^{-4}	DDX58, CDKN1A, NFKBIE, RELB, NFKBIA, MDM2, NFKB2, EIF2AK2
mmu05164, Influenza A	8	3.32×10^{-3}	DDX58, TNFRSF10B, NFKBIA, H2-DMB1, FAS, EIF2AK2, NXT2, CXCL10
mmu04068, FoxO signaling pathway	7	4.21×10^{-3}	CDKN1A, GABARAPL1, ATG12, FBXO25, MDM2, FOXO3, CCNG2
mmu04623, Cytosolic DNA-sensing pathway	5	6.03×10^{-3}	DDX58, TMEM173, RIPK3, NFKBIA, CXCL10
mmu04622, RIG-I-like receptor signaling pathway	5	7.47×10^{-3}	DDX58, TMEM173, ATG12, NFKBIA, CXCL10
mmu04142, Lysosome	6	1.27×10^{-2}	ABCB9, AP3M2, SMPD1, ARSA, SORT1, CTSF
mmu05162, Measles	6	1.95×10^{-2}	DDX58, TNFRSF10B, BBC3, NFKBIA, FAS, EIF2AK2
mmu04064 NF-kappa B signaling pathway	5	2.48×10^{-2}	DDX58, RELB, NFKBIA, NFKB2, PIDD1
mmu04210, Apoptosis	4	3.10×10^{-2}	TNFRSF10B, NFKBIA, FAS, APAF1
mmu05206, MicroRNAs in cancer	8	3.82×10^{-2}	NOTCH3, CDKN1A, RASSF1, MDM2, CCNG1, DDIT4, PDCD4, MIR34A
mmu05203, Viral carcinogenesis	7	4.85×10^{-2}	CDKN1A, KAT2B, NFKBIA, MDM2, PMAIP1, NFKB2, EIF2AK2

Table III. The top 20 biological processes associated with the differentially expressed genes overlapping between cisplatin vs. control and combination vs. control groups.

A, Downregulated genes

Term	Count	P-value	Gene name
GO:0006334, nucleosome assembly	18	$4.24x10^{-18}$	H1F0, HIST1H2BB, HIST4H4, HIST1H1C, HIST1H2AF, HIST1H1B, HIST1H2AG, HIST1H1A, HIST1H2BH, HIST2H4, etc.
GO:0031497, chromatin assembly	18	$6.98x10^{-18}$	H1F0, HIST1H2BB, HIST4H4, HIST1H1C, HIST1H2AF, HIST1H1B, HIST1H2AG, HIST1H1A, HIST1H2BH, HIST2H4, etc.
GO:0034728, nucleosome organization	18	$8.89x10^{-18}$	H1F0, HIST1H2BB, HIST4H4, HIST1H1C, HIST1H2AF, HIST1H1B, HIST1H2AG, HIST1H1A, HIST1H2BH, HIST2H4, etc.
GO:0065004, protein-DNA complex assembly	18	$8.89x10^{-18}$	H1F0, HIST1H2BB, HIST4H4, HIST1H1C, HIST1H2AF, HIST1H1B, HIST1H2AG, HIST1H1A, HIST1H2BH, HIST2H4, etc.
GO:0006323, DNA packaging	18	$1.55x10^{-15}$	H1F0, HIST1H2BB, HIST4H4, HIST1H1C, HIST1H2AF, HIST1H1B, HIST1H2AG, HIST1H1A, HIST1H2BH, HIST2H4, etc.
GO:0006333, chromatin assembly or disassembly	18	$5.73x10^{-15}$	H1F0, HIST1H2BB, HIST4H4, HIST1H1C, HIST1H2AF, HIST1H1B, HIST1H2AG, HIST1H1A, HIST1H2BH, HIST2H4, etc.
GO:0034622, cellular macromolecular complex assembly	19	$5.45x10^{-11}$	H1F0, HIST1H2BB, HIST4H4, HIST1H1C, HIST1H2AF, HIST1H1B, HIST1H2AG, HIST1H1A, HIST1H2BH, CTTNBP2, etc.
GO:0034621, cellular macromolecular complex subunit organization	19	$4.01x10^{-10}$	H1F0, HIST1H2BB, HIST4H4, HIST1H1C, HIST1H2AF, HIST1H1B, HIST1H2AG, HIST1H1A, HIST1H2BH, CTTNBP2, etc.
GO:0065003, macromolecular complex assembly	19	$6.33x10^{-8}$	H1F0, HIST1H2BB, HIST4H4, HIST1H1C, HIST1H2AF, HIST1H1B, HIST1H2AG, HIST1H1A, HIST1H2BH, CTTNBP2, etc.
GO:0006325, chromatin organization	18	$1.25x10^{-7}$	H1F0, HIST1H2BB, HIST4H4, HIST1H1C, HIST1H2AF, HIST1H1B, HIST1H2AG, HIST1H1A, HIST1H2BH, HIST2H4, etc.
GO:0043933, macromolecular complex subunit organization	19	$2.18x10^{-7}$	H1F0, HIST1H2BB, HIST4H4, HIST1H1C, HIST1H2AF, HIST1H1B, HIST1H2AG, HIST1H1A, HIST1H2BH, CTTNBP2, etc.
GO:0051276, chromosome organization	18	$3.94x10^{-6}$	H1F0, HIST1H2BB, HIST4H4, HIST1H1C, HIST1H2AF, HIST1H1B, HIST1H2AG, HIST1H1A, HIST1H2BH, HIST2H4, etc.
GO:0030855, epithelial cell differentiation	8	$5.36x10^{-4}$	SPRR1A, SPRR1B, GJA1, SPRR2G, PTCH1, ID3, FZD2, SPRR2K
GO:0007507, heart development	10	$1.09x10^{-3}$	NRP2, ID2, EDN1, GJA1, FHL2, PTCH1, ADAMTS1, ID3, MECOM, TPM1
GO:0031424, keratinization	4	$3.94x10^{-3}$	SPRR1A, SPRR1B, SPRR2G, SPRR2K
GO:0060429, epithelium development	10	$4.08x10^{-3}$	SPRR1A, LMO4, SPRR1B, GJA1, SPRR2G, PTCH1, ID3, FZD2, MECOM, SPRR2K
GO:0042325, regulation of phosphorylation	10	$6.31x10^{-3}$	SPRY1, PDGFB, SOCS3, EDN1, PDGFRB, TRIB3, CD24A, PPP1R14B, IRS1, TRIB1
GO:0019220, regulation of phosphate metabolic process	10	$7.97x10^{-3}$	SPRY1, PDGFB, SOCS3, EDN1, PDGFRB, TRIB3, CD24A, PPP1R14B, IRS1, TRIB1
GO:0051174, regulation of phosphorus metabolic process	10	$7.97x10^{-3}$	SPRY1, PDGFB, SOCS3, EDN1, PDGFRB, TRIB3, CD24A, PPP1R14B, IRS1, TRIB1
GO:0043009, chordate embryonic development	12	$9.30x10^{-3}$	HES1, SFRP2, EDN1, NLE1, PDGFRB, GJA1, PTCH1, GAS1, MECOM, TPM1, etc.

Table III. Continued.

B, Upregulated genes

Term	Count	P-value	Gene name
GO:0012501, programmed cell death	16	$1.95x10^{-5}$	TRP53INP1, FAS, DDIT4, CKAP2, ZMAT3, EDA2R, PMAIP1, PDCD4, TMEM173, NOD1, etc.
GO:0008219, cell death	16	$4.35x10^{-5}$	TRP53INP1, FAS, DDIT4, CKAP2, ZMAT3, EDA2R, PMAIP1, PDCD4, TMEM173, NOD1, etc.
GO:0016265, death	16	$5.68x10^{-5}$	TRP53INP1, FAS, DDIT4, CKAP2, ZMAT3, EDA2R, PMAIP1, PDCD4, TMEM173, NOD1, etc.
GO:0006915, apoptosis	15	$6.61x10^{-5}$	TRP53INP1, APAF1, FAS, CKAP2, ZMAT3, PMAIP1, PDCD4, DDIT4, TMEM173, NOD1, etc.
GO:0007049, cell cycle	16	$3.41x10^{-4}$	CKAP2, TXNIP, KAT2B, CCNG1, SESN2, CDKN1A, EREG, RASSF1, TRP53INP1, MDM2, etc.
GO:0007050, cell cycle arrest	5	$1.64x10^{-3}$	CDKN1A, AK1, RASSF1, TRP53INP1, SESN2
GO:0022402, cell cycle process	11	$2.67x10^{-3}$	CDKN1A, EREG, AK1, RASSF1, TRP53INP1, MDM2, SESN2, CCNG1, CCNG2, SMC4, etc.
GO:0033554, cellular response to stress	11	$3.25x10^{-3}$	POLK, CLSPN, CDKN1A, ERCC5, ATG9B, ATG12, BTG2, ZMAT3, PMAIP1, EIF2AK2, etc.
GO:0012502, induction of programmed cell death	7	$3.78x10^{-3}$	NOD1, RIPK3, TRP53INP1, PMAIP1, FAS, APAF1, PHLDA3
GO:0006917, induction of apoptosis	7	$3.78x10^{-3}$	NOD1, RIPK3, TRP53INP1, PMAIP1, FAS, APAF1, PHLDA3
GO:0043068, positive regulation of programmed cell death	8	$7.02x10^{-3}$	CDKN1A, NOD1, RIPK3, TRP53INP1, PMAIP1, FAS, APAF1, PHLDA3
GO:0010942, positive regulation of cell death	8	$7.32x10^{-3}$	CDKN1A, NOD1, RIPK3, TRP53INP1, PMAIP1, FAS, APAF1, PHLDA3
GO:0006974, response to DNA damage stimulus	8	$1.43x10^{-2}$	POLK, CLSPN, CDKN1A, ERCC5, BTG2, ZMAT3, PMAIP1, PHLDA3
GO:0045596, negative regulation of cell differentiation	6	$2.33x10^{-2}$	NOTCH3, EREG, GDF11, NFKBIA, RC3H1, TOB1
GO:0043065, positive regulation of apoptosis	7	$2.35x^{1}0^{-2}$	NOD1, RIPK3, TRP53INP1, PMAIP1, FAS, APAF1, PHLDA3
GO:0008104, protein localization	13	$3.59x10^{-2}$	ARL6IP1, TXNIP, GDI1, ABCB9, CHMP5, ZMAT3, NFKBIA, PMAIP1, OPTN, CXCL10, etc.
GO:0007033, vacuole organization	3	$3.67x10^{-2}$	ATG9B, ATG12, CHMP5
GO:0009411, response to UV	3	$3.87x10^{-2}$	CDKN1A, ERCC5, PMAIP1

GO, Gene Ontology.

cytotoxicity, DNA damage and apoptosis in cochlear hair cells contribute to cisplatin-associated ototoxicity (10,12-14). The present study demonstrated that cisplatin-induced ototoxicity in HEI-OC1 auditory cells was associated with the inhibition of cell viability and dysregulation of genes related to apoptosis, cell cycle arrest and several pathways, including the p53, HIF-1, Wnt and PI3K-Akt signaling pathways. Treatment with Tet protected HEI-OC1 auditory cells against cisplatin-induced cytotoxicity *in vitro* and regulated several signaling pathways.

The synergistic effect of Tan IIA on cisplatin-induced cytotoxicity in cancer cells has been previously reported (18). Indeed, Tan IIA was previously observed to enhance cisplatin-induced apoptosis and cell cycle arrest at the S phase in human prostate cancer cells (18). In another study, Tan IIA promoted apoptosis and cell cycle arrest at the sub-G_1 phase in human hepatocellular carcinoma cells (19). Du *et al* (16) demonstrated that 24-h Tan IIA treatments at concentrations <64 mg/l could alleviate radiation-induced cytotoxicity and apoptosis of HEI-OC1 auditory cells by inhibiting p65/nuclear factor κB p53 and p21 signaling pathways. Du *et al* (16) also indicated that Tan IIA at concentrations >16 mg/l resulted in significant cytotoxicity, whereas Tan IIA <8 mg/l had no cytotoxic effects on HEI-OC1 cells. However, the present study determined that Tan IIA concentrations as low as 1.5 mg/l augmented the effect of cisplatin on cell viability of HEI-OC1 auditory cells. This difference might be due to the longer treatment period in the present study, compared with Du *et al* (16) (30 and 24 h, respectively). Thus, it may be hypothesized that

Table IV. Kyoto Encyclopedia of Genes and Genomes (KEGG) pathways associated with the differentially expressed genes overlapping between cisplatin vs. control and combination vs. control groups.

A, Downregulated genes

Term	Count	P-value	Gene name
mmu05322, Systemic lupus erythematosus	14	3.29×10^{-10}	HIST1H2BB, HIST4H4, HIST1H2AF, HIST1H2AG, HIST1H2BH, HIST2H4, HIST1H2BM, HIST1H4A, H3F3B, H2AFX, etc.
mmu04510, Focal adhesion	9	3.42×10^{-3}	GM12715, PDGFB, COL3A1, COL1A2, PDGFRB, COL6A1, THBS1, COL5A3, SPP1
mmu04512, ECM-receptor interaction	6	3.90×10^{-3}	COL3A1, COL1A2, COL6A1, THBS1, COL5A3, SPP1
mmu04330, Notch signaling pathway	4	2.53×10^{-2}	DTX4, HES1, MAML3, LFNG

B, Upregulated genes

Term	Count	P-value	Gene name
mmu04115, p53 signaling pathway	10	6.27×10^{-9}	CDKN1A, ZMAT3, MDM2, PMAIP1, FAS, APAF1, SESN2, CCNG1, CCNG2, GTSE1
mmu04623, Cytosolic DNA-sensing pathway	5	1.35×10^{-3}	DDX58, TMEM173, RIPK3, NFKBIA, CXCL10
mmu04622, RIG-I-like receptor signaling pathway	5	2.97×10^{-3}	DDX58, TMEM173, ATG12, NFKBIA, CXCL10
mmu04210, Apoptosis	4	4.16×10^{-2}	TNFRSF10B, NFKBIA, FAS, APAF1

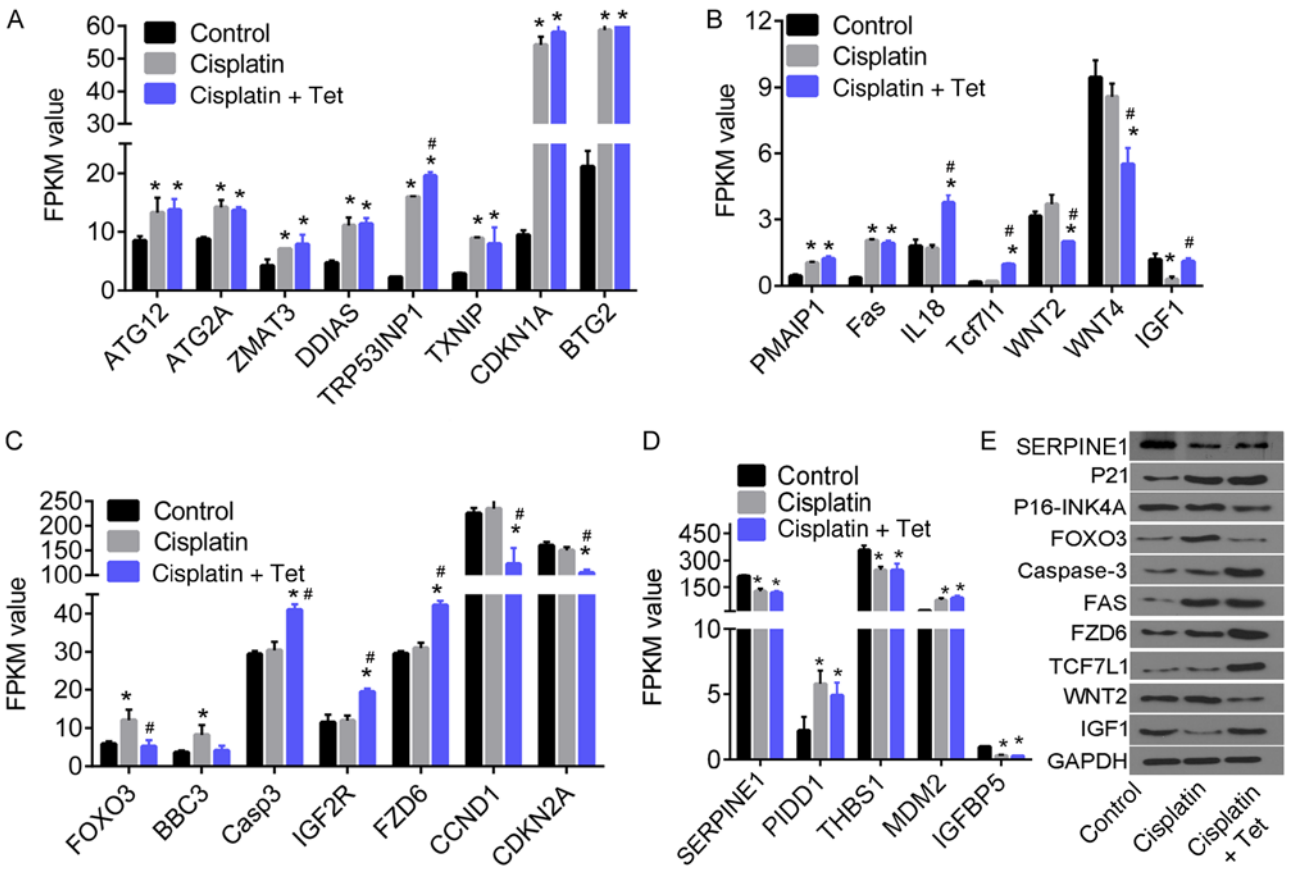

Figure 5. FPKM values and expression of several DEGs in the three groups. (A-D) FPKM values of several random selected up- or downregulated DEGs with typical expression profiling in response to treatment with cisplatin alone or combined with Tet. (E) Expression of several protein products of DEGs. *P<0.05, vs. control. #P<0.05 vs. Cisplatin. The differences were analyzed by one-way ANOVA followed by Tukey's post hoc test. DEG, differentially expressed gene; FKPM, fragments per kilobase of exon model per million reads mapped.

Table V. The top 20 biological processes associated with the differentially expressed genes induced by combination treatment compared with control.

Downregulated genes			
Term	Count	P-value	Gene name
GO:0006334, nucleosome assembly	19	3.03×10^{-14}	HIST1H2AB, HIST4H4, HIST1H4K, HIST1H2AF, HIST1H2AG, HIST1H2BM, HIST1H2BK, HIST1H4A, HIST1H4B, HIST2H2AC, etc.
GO:0031497, chromatin assembly	19	5.06×10^{-14}	HIST1H2AB, HIST4H4, HIST1H4K, HIST1H2AF, HIST1H2AG, HIST1H2BM, HIST1H2BK, HIST1H4A, HIST1H4B, HIST2H2AC, etc.
GO:0065004, protein-DNA complex assembly	19	6.50×10^{-14}	HIST1H2AB, HIST4H4, HIST1H4K, HIST1H2AF, HIST1H2AG, HIST1H2BM, HIST1H2BK, HIST1H4A, HIST1H4B, HIST2H2AC, etc.
GO:0034728, nucleosome organization	19	6.50×10^{-14}	HIST1H2AB, HIST4H4, HIST1H4K, HIST1H2AF, HIST1H2AG, HIST1H2BM, HIST1H2BK, HIST1H4A, HIST1H4B, HIST2H2AC, etc.
GO:0034622, cellular macromo lecular complex assembly	28	6.42×10^{-13}	EIF6, FKBP4, WNT2, HIST1H2BM, HIST1H4A, PRMT5, TUBA1C, NIP7, HIST1H1A, HIST1H2BH, FLNA, etc.
GO:0042254, ribosome biogenesis	20	7.62×10^{-12}	EIF6, NAF1, EXOSC4, NIP7, BOP1, IMP3, CDKN2A, NPM1, RRS1, NHP2, etc.
GO:0034470, ncRNA processing	23	9.92×10^{-12}	NAF1, BOP1, RRP9, QTRT1, EXOSC1, TRMT61A, FBL, IMP3, NOP2, CDKN2A, etc.
GO:0006323, DNA packaging	19	1.16×10^{-11}	HIST1H2AB, HIST4H4, HIST1H4K, HIST1H2AF, HIST1H2AG, HIST1H2BM, HIST1H2BK, HIST1H4A, HIST1H4B, HIST2H2AC, etc.
GO:0034621, cellular macromolecular complex subunit organization	28	1.17×10^{-11}	HIST1H2AB, EIF6, FKBP4, WNT2, CTTNBP2, NIP7, FLNA, HIST2H4, HIST1H3A, CACNA1A, etc.
GO:0022613, ribonucleoprotein complex biogenesis	21	3.69×10^{-11}	EIF6, NAF1, RRP9, FBL, IMP3, NOP2, CDKN2A, PRMT5, NPM1, RRS1, etc.
GO:0006333, chromatin assembly or disassembly	19	4.39×10^{-11}	HIST1H2AB, HIST4H4, HIST1H4K, HIST1H2AF, HIST1H2AG, HIST1H2BM, HIST1H2BK, HIST1H4A, HIST1H4B, HIST2H2AC, etc.
GO:0034660, ncRNA metabolic process	24	2.17×10^{-10}	NAF1, PUS1, EXOSC4, BOP1, QTRT1, EXOSC1, TRMT61A, IMP3, CDKN2A, METTL1, etc.
GO:0065003, macromolecular complex assembly	30	8.60×10^{-10}	HIST4H4, FKBP4, WNT2, CTTNBP2, PRMT5, NPM1, MYC, TUBA1C, NIP7, FLNA, etc.
GO:0043933, macromolecular complex subunit organization	30	5.71×10^{-9}	HIST1H2AB, EIF6, FKBP4, WNT2, CTTNBP2, PRMT5, NPM1, MYC, NIP7, etc.
GO:0006364, rRNA processing	13	9.96×10^{-8}	NAF1, EXOSC4, EXOSC1, BOP1, FBL, RCL1, IMP3, NOP2, CDKN2A, NHP2, etc.
GO:0016072, rRNA metabolic process	13	1.16×10^{-7}	NAF1, EXOSC4, EXOSC1, BOP1, FBL, RCL1, IMP3, NOP2, CDKN2A, NHP2, etc.
GO:0006396, RNA processing	29	8.47×10^{-7}	NAF1, BOP1, QTRT1, IMP3, CDKN2A, METTL1, PRMT5, TSEN2, EXOSC4, RPP40, etc.
GO:0008033, tRNA processing	11	3.90×10^{-6}	PUS7L, ELAC2, PUS1, METTL1, WDR4, QTRT1, TSEN2, TRMT61A, NSUN2, FBL, etc.
GO:0006399, tRNA metabolic process	12	5.36×10^{-5}	PUS7L, ELAC2, PUS1, METTL1, WDR4, QTRT1, TSEN2, TRMT61A, RPP40, FBL, etc.
GO:0006325, chromatin organization	20	1.14×10^{-4}	HIST1H2AB, PRMT5, H2AFZ, H1F0, HIST1H2BB, HIST1H1C, HIST1H1B, HIST1H1A, HIST1H2BH, HIST2H4, etc.

Table V. Continued.

Upregulated genes			
Term	Count	P-value	Gene name
GO:0012501, programmed cell death	21	$1.23x10^{-5}$	CKAP2, ZMAT3, PMAIP1, BCL2L11, DDIT4, TMEM173, CASP3, TRP53INP1, FAS, PHLDA3, etc.
GO:0007049, cell cycle	24	$1.75x10^{-5}$	TXNIP, CKAP2, NUSAP1, CCNG1, NCAPD3, BRCA1, CDKN1A, RASSF1, TRP53INP1, MDM2, etc.
GO:0012502, induction of programmed cell death	12	$2.50x10^{-5}$	SERINC3, CASP3, CASP4, NOD1, IL18, RIPK3, TRP53INP1, PMAIP1, FAS, APAF1, etc.
GO:0006917, induction of apoptosis	12	$2.50x10^{-5}$	SERINC3, CASP3, CASP4, NOD1, IL18, RIPK3, TRP53INP1, PMAIP1, FAS, APAF1, etc.
GO:0006915, apoptosis	20	$3.28x10^{-5}$	CKAP2, ZMAT3, PMAIP1, PDCD4, DDIT4, CASP3, TMEM173, TRP53INP1, JAK2, FAS, etc.
GO:0008219, cell death	21	$3.32x10^{-5}$	JAK2, FAS, CKAP2, ZMAT3, EDA2R, PMAIP1, DDIT4, TMEM173, CASP3, TRP53INP1, etc.
GO:0022402, cell cycle process	18	$4.28x10^{-5}$	NUSAP1, CCNG1, SESN2, CCNG2, NCAPD3, BRCA1, CDKN1A, RASSF1, TRP53INP1, MDM2, etc.
GO:0016265, death	21	$4.61x10^{-5}$	TRP53INP1, JAK2, FAS, CKAP2, ZMAT3, PMAIP1, PDCD4, TAX1BP1, BCL2L11, DDIT4, etc.
GO:0043068, positive regulation of programmed cell death	14	$5.61x10^{-5}$	PMAIP1, BCL2L11, BRCA1, SERINC3, CDKN1A, CASP3, CASP4, NOD1, TRP53INP1, FAS, etc.
GO:0010942, positive regulation of cell death	14	$6.06x10^{-5}$	PMAIP1, BCL2L11, BRCA1, SERINC3, CDKN1A, CASP3, CASP4, NOD1, TRP53INP1, FAS, etc.
GO:0043065, positive regulation of apoptosis	13	$2.13x10^{-4}$	PMAIP1, BCL2L11, BRCA1, SERINC3, CASP3, RIPK3, TRP53INP1, APAF1, FAS, PHLDA3, etc.
GO:0007050, cell cycle arrest	6	$1.23x10^{-3}$	GAS2L3, CDKN1A, AK1, RASSF1, TRP53INP1, SESN2
GO:0042981, regulation of apoptosis	18	$2.19x10^{-3}$	IL18, PMAIP1, TAX1BP1, BRCA1, SERINC3, CASP3, CDKN1A, BTG2, TRP53INP1, FAS, etc.
GO:0043067, regulation of programmed cell death	18	$2.49x10^{-3}$	IL18, PMAIP1, TAX1BP1, BRCA1, SERINC3, CASP3, CDKN1A, BTG2, TRP53INP1, FAS, etc.
GO:0010941, regulation of cell death	18	$2.63x10^{-3}$	IL18, PMAIP1, TAX1BP1, BRCA1, SERINC3, CASP3, CDKN1A, BTG2, TRP53INP1, FAS, etc.
GO:0007076, mitotic chromosome condensation	3	$3.98x10^{-3}$	NUSAP1, NCAPD3, SMC4
GO:0033554, cellular response to stress	14	$4.91x10^{-3}$	POLK, ATG9B, ATG12, NEIL3, ZMAT3, PMAIP1, BRCA1, CASP3, CDKN1A, BTG2, etc.
GO:0007067, mitosis	9	$5.62x10^{-3}$	SPC25, KNTC1, NUSAP1, NDC80, CEP55, CCNG1, CCNG2, NCAPD3, SMC4
GO:0000280, nuclear division	9	$5.62x10^{-3}$	SPC25, KNTC1, NUSAP1, NDC80, CEP55, CCNG1, CCNG2, NCAPD3, SMC4
GO:0000087, M phase of mitotic cell cycle	9	$6.38x10^{-3}$	SPC25, KNTC1, NUSAP1, NDC80, CEP55, CCNG1, CCNG2, NCAPD3, SMC4

GO, Gene Ontology.

Tan IIA-induced cytotoxicity to HEI-OC1 auditory cells is time-dependent, since the concentration used in the present study was far below the IC_{50} value of 151.8 mg/l.

By contrast, low concentrations of Tet (37.5 and 70 mg/l) exerted a protective effect against cisplatin-induced cytotoxicity. RNA-seq analysis was carried out to examine the underlying molecular mechanism. Cisplatin inhibited the viability of HEI-OC1 auditory cells by decreasing the expression of Hist1 and Hist2 gene clusters that are associated with DNA replication and actively transcribed in differentiating cells (20). Cisplatin also inhibited the expression of genes related to cell migration and proliferation, including IGF1 and IGFBP5. The expression of IGF1, IGF receptors and IGFBPs has been reported to induce or promote the

Table VI. Kyoto Encyclopedia of Genes and Genomes pathways associated with the differentially expressed genes induced by combination treatment compared with control.

A, Downregulated genes

Term	Count	P-value	Gene name
mmu05322, Systemic lupus erythematosus	15	$1.94x10^{-7}$	HIST1H2AB, HIST4H4, HIST1H4K, HIST1H2AF, HIST1H2AG, HIST1H2BM, HIST1H2BK, HIST1H4A, HIST1H4B, HIST2H2AC, etc.
mmu03010, Ribosome	10	$3.36x10^{-4}$	RPS19, RPL41, RPLP1, GM10020, RPL26, RPL3, RPL10, RPL36, RPL37, RPS5
mmu04510, Focal adhesion	15	$3.76x10^{-4}$	PDGFB, COL3A1, COL2A1, COL5A3, FLNA, CCND1, COL1A2, PDGFRB, THBS1, SPP1, etc.
mmu00670, One carbon pool by folate	4	$6.69x10^{-3}$	SHMT2, ATIC, MTHFD1L, GART
mmu00100, Steroid biosynthesis	4	$7.98x10^{-3}$	CYP51, SQLE, LSS, DHCR24
mmu04512, ECM-receptor interaction	7	$1.69x10^{-2}$	COL3A1, COL1A2, COL6A1, COL2A1, THBS1, COL5A3, SPP1

B, Upregulated genes

Term	Count	P-value	Gene name
mmu04115, p53 signaling pathway	11	$3.09x10^{-8}$	CDKN1A, CASP3, ZMAT3, MDM2, PMAIP1, FAS, APAF1, SESN2, CCNG1, CCNG2, etc.
mmu04623, Cytosolic DNA-sensing pathway	7	$1.10x10^{-4}$	DDX58, TMEM173, IL18, RIPK3, NFKBIA, CHUK, CXCL10
mmu05200, Pathways in cancer	13	$1.74x10^{-3}$	NFKBIA, TCF7L1, FZD6, CTNNA2, CASP3, CDKN1A, RASSF1, MDM2, WNT9A, FAS, etc.
mmu04622, RIG-I-like receptor signaling pathway	6	$2.57x10^{-3}$	DDX58, TMEM173, ATG12, NFKBIA, CHUK, CXCL10
mmu04210, Apoptosis	6	$7.41x10^{-3}$	CASP3, TNFRSF10B, NFKBIA, FAS, APAF1, CHUK
mmu04621, NOD-like receptor signaling pathway	5	$1.11x10^{-2}$	NOD1, IL18, NFKBIA, TAB2, CHUK
mmu04920, Adipocytokine signaling pathway	5	$1.44x10^{-2}$	CPT1C, NFKBIE, NFKBIA, JAK2, CHUK
mmu04142, Lysosome	6	$2.59x10^{-2}$	SGSH, ABCB9, AP3M2, IGF2R, SORT1, CTSF
mmu05215, Prostate cancer	5	$3.77x10^{-2}$	CDKN1A, MDM2, NFKBIA, TCF7L1, CHUK

proliferation of various cell types through several signaling pathways, such as PI3K/Akt (21-23). It has been demonstrated that IGF1 could counteract cisplatin-induced DNA damage by inhibiting cisplatin-induced phosphorylation of histone H2AX and ataxia-telangiectasia mutated, and blocking DNA double-strand break repair (24). IGFBP5 overexpression and IGF1R inhibition are associated with increased cisplatin sensitivity in esophageal carcinoma cells, lung and ovarian cancer cells (25-27). The present study demonstrated that, compared with cisplatin alone, Tet treatment increased the expression of IGF1, but not IGFBP5. These results suggested that Tet protected HEI-OC1 auditory cells from cisplatin-induced cytotoxicity by restoring IGF1 signaling.

Exposure to cisplatin upregulated genes that were associated with apoptosis and autophagy, including ATG12, ZMAT3, PMAIP1, TRP53INP1 and PIDD1. However, the expression of these genes was not modulated by Tet treatment. By contrast, treatment with Tet downregulated FOXO3 (significantly) and BBC3 (insignificantly), compared with cisplatin alone. A previous study demonstrated that the proapoptotic FoxO signaling pathway was activated by amikacin-induced ototoxicity (28). FOXO3 mediates a chemo-protection effect in advanced cancer by interacting with TP53 and mutations in TP53 prevent FOXO3 binding, thereby enhancing FOXO3-induced cell death in high-stage neuroblastoma (29). Additionally, FOXO3 links autophagy and apoptosis by regulating the transactivation of the proapoptotic gene BBC3 (30). Under the condition of autophagy inhibition, BBC3 is transactivated by FOXO3 (29,30). In the present study, the expression of FOXO3 and BBC3 following cisplatin exposure was increased, consistent with increased apoptosis. It could be hypothesized that increased FOXO3 and BB3-mediated apoptosis may be associated with inhibition of autophagy following cisplatin treatment. Moreover, the protective effect of Tet treatment might be mediated by modulation of autophagy.

The proapoptotic p53 signaling pathway is activated in the cochlea and in HEI-OC1 auditory cells following cisplatin exposure (8,10,31,32). Xiong *et al* (32) and Ma *et al* (31) indicated that the expression or acetylation of p53 in HEI-OC1 auditory cells could be increased by cisplatin treatment, thereby promoting apoptosis. In particular, Ma *et al* (31) demonstrated that ginkgolide B prevented cisplatin-induced cytotoxicity and decreased p53 expression in cisplatin-treated cochlear cells. Moreover, Benkafadar *et al* (33) suggested that the knockdown of p53 could attenuate cisplatin-induced ototoxicity and cochlear cell apoptosis. Consistent with these previous reports, the present study demonstrated that cisplatin induced significant upregulation of p53 signaling-related genes, including ZMAT3, PMAIP1, TRP53INP1 and PIDD1. However, the expression of these genes was not affected by Tet treatment, indicating that the protective effect of Tet on HEI-OC1 auditory cells did not involve p53 signaling.

A previous study suggested that the Wnt signaling pathway protects against neomycin-induced hair cell damage (9). Liu *et al* (9) demonstrated that β-catenin activation prevented apoptosis of hair cells. By contrast, inhibition of β-catenin increased FOXO3 expression, ROS production, and apoptosis in these cells (9). In addition, the inhibition of Wnt signaling in spiral ganglion neurons may increase the levels of ROS (8). The present study suggested that Tet addition into HEI-OC1 auditory cells increased the expression of two mediators of the Wnt signaling pathway, including TCF7L1 and FZD6. Thus, activation of Wnt signaling may be involved in the Tet-mediated protective effect on HEI-OC1 auditory cells. However, this study demonstrated that WNT2 and WNT4 genes, which are necessary for the activation of FZD6, were downregulated specifically by combination with Tet. These results suggested that the activation of Wnt signaling may be mediated by novel factors, rather than WNT2/4.

The present study has limitations. Firstly, the concentrations of cisplatin used in this study were too low. To minimize its cytotoxicity *in vitro*, cells were treated with cisplatin and Tet at concentrations $<IC_{50}$ values. Obvious reverse changes in cell viability and genomics were observed between combination treatment of 37.5 mg/l Tet and 30 μM cisplatin, and 30 μM cisplatin alone. Moreover, the potential mechanisms underlying the role of Tet were only identified using RNA-seq and bioinformatics analysis. Experimental validation would provide further insight into the molecular basis of Tet-mediated inhibition of ototoxicity.

In conclusion, the present study confirmed that low doses of Tet could attenuate cisplatin-induced cytotoxicity in HEI-OC1 auditory cells. Gene expression analysis suggested that cisplatin induced ototoxicity *in vitro* by activating the p53 and FoxO signaling pathways, and inhibiting IGF signaling. Tet attenuated ototoxicity through activation of the Wnt/β-catenin and IGF pathways, and inhibition of FOXO3/BBC3 signaling. Further validation is required to directly demonstrate the roles of these pathways in auditory cells.

Acknowledgements

The authors would like to thank Professor Federico Kalinec (David Geffen School of Medicine at UCLA, CA, USA) for the generous donation of the HEI-OC1 auditory cells.

Funding

No funding was received.

Availability of data and materials

All data generated or analyzed during this study are included in this published article. The fastq files of raw sequencing data are available from the corresponding author upon reasonable request.

Authors' contributions

GG and XT designed the study. GG, XH, JC and LB acquired, analyzed and interpreted the data. XH, JC and LB carried out the statistical analysis.GG drafted the manuscript. XH and XT revised the manuscript for important intellectual content. All authors read and approved the final manuscript.

Ethics approval and consent to participate

Not applicable.

Patient consent for publication

Not applicable.

Competing interests

The authors declare that they have no competing interests.

References

1. Breglio AM, Rusheen AE, Shide ED, Fernandez KA, Spielbauer KK, McLachlin KM, Hall MD, Amable L and Cunningham LL: Cisplatin is retained in the cochlea indefinitely following chemotherapy. Nat Commun 8: 1654, 2017.
2. Shorter P, Harden F, Owen R, Panizza B, Burmeister B, Sommerville J, Mengersen K and Foote M: Risk profiles for sensorineural hearing loss in patients with head and neck cancer receiving cisplatin-based chemoradiation. J Med Imaging Radiat Sci 48: 61-67, 2017.
3. Wang J, Chen YY, Tai A, Chen XL, Huang SM, Yang C, Bao Y, Li NW, Deng XW, Zhao C, *et al*: Sensorineural hearing loss after combined intensity modulated radiation therapy and cisplatin-based chemotherapy for nasopharyngeal carcinoma. Transl Oncol 8: 456-462, 2015.
4. Robertson MS, Hayashi SS, Camet ML, Trinkaus K, Henry J and Hayashi RJ: Asymmetric sensorineural hearing loss is a risk factor for late-onset hearing loss in pediatric cancer survivors following cisplatin treatment. Pediatr Blood Cancer 66: e27494, 2019.
5. Bass JK, Hua CH, Huang J, Onar-Thomas A, Ness KK, Jones S, White S, Bhagat SP, Chang KW and Merchant TE: Hearing loss in patients who received cranial radiation therapy for childhood cancer. J Clin Oncol 34: 1248-1255, 2016.
6. Wu X, Li X, Song Y, Li H, Bai X, Liu W, Han Y, Xu L, Li J, Zhang D, *et al*: Allicin protects auditory hair cells and spiral ganglion neurons from cisplatin-Induced apoptosis. Neuropharmacology 116: 429-440, 2017.
7. Sheth S, Mukherjea D, Rybak LP and Ramkumar V: Mechanisms of cisplatin-induced ototoxicity and otoprotection. Front Cell Neurosci 11: 338, 2017.
8. Liu W, Xu X, Fan Z, Sun G, Han Y, Zhang D, Xu L, Wang M, Wang X, Zhang S, *et al*: Wnt signaling activates TP53-induced glycolysis and apoptosis regulator and protects against cisplatin-induced spiral ganglion neuron damage in the mouse cochlea. Antioxid Redox Signal 30: 1389-1410, 2019.
9. Liu L, Chen Y, Qi J, Zhang Y, He Y, Ni W, Li W, Zhang S, Sun S, Taketo MM, *et al*: Wnt activation protects against neomycin-induced hair cell damage in the mouse cochlea. Cell Death Dis 7: e2136, 2016.

10. Guo X, Bai X, Li L, Li J and Wang H: Forskolin protects against cisplatin-induced ototoxicity by inhibiting apoptosis and ROS production. Biomed Pharmacother 99: 530-536, 2018.
11. Zhang Q, Liu H, McGee J, Walsh EJ, Soukup GA and He DZ: Identifying microRNAs involved in degeneration of the organ of corti during age-related hearing loss. PLoS One 8: e62786, 2013.
12. Wang P, Zhang P, Huang J, Li M and Chen X: Trichostatin a protects against cisplatin-induced ototoxicity by regulating expression of genes related to apoptosis and synaptic function. Neurotoxicology 37: 51-62, 2013.
13. Bhatta P, Dhukhwa A, Sheehan K, Al Aameri RFH, Borse V, Ghosh S, Sheth S, Mamillapalli C, Rybak L, Ramkumar V and Mukherjea D: Capsaicin protects against cisplatin ototoxicity by changing the STAT3/STAT1 ratio and activating Cannabinoid (CB2) receptors in the Cochlea. Sci Rep 9: 4131, 2019.
14. Kitcher SR, Kirkwood NK, Camci ED, Wu P, Gibson RM, Redila VA, Simon JA, Rubel EW, Raible DW, Richardson GP and Kros CJ: ORC-13661 protects sensory hair cells from aminoglycoside and cisplatin ototoxicity. JCI Insight 4: e126764, 2019.
15. Cui C, Liu D and Qin X: Attenuation of streptomycin ototoxicity by tetramethylpyrazine in guinea pig cochlea. Otolaryngol Head Neck Surg 152: 904-911, 2015.
16. Du S, Yao Q, Tan P, Xie G, Ren C, Sun Q, Zhang X, Zheng R, Yang K, Yuan Y and Yuan Q: Protective effect of tanshinone IIA against radiation-induced ototoxicity in HEI-OC1 cells. Oncol Lett 6: 901-906, 2013.
17. Bayram A, Kaya A, Akay E, Hıra İ and Özcan İ: The protective role of tetramethylpyrazine against cisplatin-induced ototoxicity. Int J Pediatr Otorhinolaryngol 94: 1-7, 2017.
18. Hou LL, Xu QJ, Hu GQ and Xie SQ: Synergistic antitumor effects of tanshinone II A in combination with cisplatin via apoptosis in the prostate cancer cells. Yao Xue Xue Bao 48: 675-679, 2013 (In Chinese).
19. Chang TW, Lin CY, Tzeng YJ and Lur HS: Synergistic combinations of tanshinone IIA and trans-resveratrol toward cisplatin-comparable cytotoxicity in HepG2 human hepatocellular carcinoma cells. Anticancer Res 34: 5473-5480, 2014.
20. Banday AR, Baumgartner M, Al Seesi S, Karunakaran DK, Venkatesh A, Congdon S, Lemoine C, Kilcollins AM, Mandoiu I, Punzo C and Kanadia RN: Replication-dependent histone genes are actively transcribed in differentiating and aging retinal neurons. Cell Cycle 13: 2526-2541, 2014.
21. Kadri Z, Lefevre C, Goupille O, Penglong T, Granger-Locatelli M, Fucharoen S, Maouche-Chretien L, Leboulch P and Chretien S: Erythropoietin and IGF-1 signaling synchronize cell proliferation and maturation during erythropoiesis. Genes Dev 29: 2603-2616, 2015.
22. Yu M, Wang H, Xu Y, Yu D, Li D, Liu X and Du W: Insulin-like growth factor-1 (IGF-1) promotes myoblast proliferation and skeletal muscle growth of embryonic chickens via the PI3K/Akt signalling pathway. Cell Biol Int 39: 910-922, 2015.
23. Bruchim I, Attias Z and Werner H: Targeting the IGF1 axis in cancer proliferation. Expert Opin Ther Targets 3: 1179-1192, 2009.
24. Jeon JH, Kim SK, Kim HJ, Chang J, Ahn CM and Chang YS: Insulin-like growth factor-1 attenuates cisplatin-induced gammaH2AX formation and DNA double-strand breaks repair pathway in non-small cell lung cancer. Cancer Lett 272: 232-241, 2008.
25. Du J, Shi HR, Ren F, Wang JL, Wu QH, Li X and Zhang RT: Inhibition of the IGF signaling pathway reverses cisplatin resistance in ovarian cancer cells. BMC Cancer 17: 851, 2017.
26. Sun Y, Zheng S, Torossian A, Speirs CK, Schleicher S, Giacalone NJ, Carbone DP, Zhao Z and Lu B: Role of insulin-like growth factor-1 signaling pathway in cisplatin-resistant lung cancer cells. Int J Radiat Oncol Biol Phys 82: e563-e572, 2012.
27. Chan D, Zhou Y, Chui CH, Lam KH, Law S, Chan AS, Li X, Lam AK and Tang JCO: Expression of insulin-like growth factor binding protein-5 (IGFBP5) reverses cisplatin-resistance in esophageal carcinoma. Cells 7: 143, 2018.
28. Liu S, Zhang X, Sun M, Xu T and Wang A: FoxO3a plays a key role in the protective effects of pomegranate peel extract against amikacin-induced ototoxicity. Int J Mol Med 40: 175-181, 2017.
29. Rupp M, Hagenbuchner J, Rass B, Fiegl H, Kiechl-Kohlendorfer U, Obexer P and Ausserlechner MJ: FOXO3-mediated chemo-protection in high-stage neuroblastoma depends on wild-type TP53 and SESN3. Oncogene 36: 6190-6203, 2017.
30. Fitzwalter BE and Thorburn A: FOXO3 links autophagy to apoptosis. Autophagy 14: 1467-1468, 2018.
31. Ma W, Li J, Hu J, Cheng Y, Wang J, Zhang X and Xu M: MiR214-regulated p53-NOX4/p66shc pathway plays a crucial role in the protective effect of Ginkgolide B against cisplatin-induced cytotoxicity in HEI-OC1 cells. Chem Biol Interact 245: 72-81, 2016.
32. Xiong H, Pang J, Yang H, Dai M, Liu Y, Ou Y, Huang Q, Chen S, Zhang Z, Xu Y, *et al*: Activation of miR-34a/SIRT1/p53 signaling contributes to cochlear hair cell apoptosis: Implications for age-related hearing loss. Neurobiol Aging 36: 1692-1701, 2015.
33. Benkafadar N, Menardo J, Bourien J, Nouvian R, François F, Decaudin D, Maiorano D, Puel JL and Wang J: Reversible p53 inhibition prevents cisplatin ototoxicity without blocking chemotherapeutic efficacy. EMBO Mol Med 9: 7-26, 2017.